

Oxidative stress pathways involved in cytotoxicity and genotoxicity of titanium dioxide (TiO2) nanoparticles on cells constitutive of alveolo-capillary barrier in vitro

Maité Hanot-Roy, Emilie Tubeuf, Ariane Guilbert, Anne Bado-Nilles, Pascale Vigneron, Bénédicte Trouiller, Anne Braun, Ghislaine Lacroix

▶ **To cite this version:**

Maité Hanot-Roy, Emilie Tubeuf, Ariane Guilbert, Anne Bado-Nilles, Pascale Vigneron, et al.. Oxidative stress pathways involved in cytotoxicity and genotoxicity of titanium dioxide (TiO2) nanoparticles on cells constitutive of alveolo-capillary barrier in vitro. Toxicology in Vitro, 2016, 33, pp.125-135. 10.1016/j.tiv.2016.01.013 . ineris-01862936v2

HAL Id: ineris-01862936
https://ineris.hal.science/ineris-01862936v2

Submitted on 31 Aug 2018

HAL is a multi-disciplinary open access archive for the deposit and dissemination of scientific research documents, whether they are published or not. The documents may come from teaching and research institutions in France or abroad, or from public or private research centers.

L'archive ouverte pluridisciplinaire **HAL**, est destinée au dépôt et à la diffusion de documents scientifiques de niveau recherche, publiés ou non, émanant des établissements d'enseignement et de recherche français ou étrangers, des laboratoires publics ou privés.

ACCEPTED MANUSCRIPT

*O*xidative stress pathways involved in cytotoxicity and genotoxicity of titanium dioxide (TiO_2) nanoparticles on cells constitutive of alveolo-capillary barrier *in vitro*.

Maïté Hanot-Roy[1,2], MHR

Emilie Tubeuf[1], ET

Ariane Guilbert[1], AG

Anne Bado-Nilles[3], ABN

Pascale Vigneron[2], PV

Bénédicte Trouiller[1], BT

Anne Braun[1], AB

Ghislaine Lacroix[1]. GL

(1) Institut National de l'Environnement Industriel et des Risques (INERIS), Unité de Toxicologie Expérimentale, Parc Technologique ALATA - BP 2, F-60550 Verneuil-en-Halatte, France,

(2) Université de Technologie de Compiègne (UTC), Laboratoire BioMécanique et BioIngénierie (BMBI), UMR CNRS 7338, 60205 Compiègne, France.

(3) Institut National de l'Environnement Industriel et des Risques (INERIS), Unité d'Ecotoxicologie in vitro et in vivo, Parc Technologique ALATA - BP 2, F-60550 Verneuil-en-Halatte, France

Corresponding author :

Maïté Hanot-Roy

maite.hanot@free.fr

0333 44 55 61 63

INERIS

Parc ALATA

Rue Jacques Taffanel

ACCEPTED MANUSCRIPT

60550 Verneuil-en-Halatte

Abstract

The health risks of nanoparticles remain a serious concern given their prevalence from industrial and domestic use. The primary route of titanium dioxide nanoparticles exposure is inhalation. The extent to which nanoparticles contribute to cellular toxicity is known to associate induction of oxidative stress. To investigate this problem further, the effect of titanium dioxide nanoparticles was examined on cell lines representative of alveolo-capillary barrier.

The present study showed that all nanoparticles-exposed cell lines displayed ROS generation. Macrophage-like THP-1 and HPMEC-ST1.6R microvascular cells were sensitive to endogenous redox changes and underwent apoptosis, but not alveolar epithelial A549 cells. Genotoxic potential of titanium dioxide nanoparticles was investigated using the activation of γH2AX, activation of DNA repair proteins and cell cycle arrest. In the sensitive cell lines, DNA damage was persistent and activation of DNA repair pathways was observed. Moreover, western blot analysis showed that specific pathways associated with cellular stress response were activated concomitantly with DNA repair or apoptosis.

Nanoparticles-induced oxidative stress is finally signal transducer for further physiological effects including genotoxicity and cytotoxicity. Within activated pathways, HSP27 and SAPK/JNK proteins appeared as potential biomarkers of intracellular stress and of sensitivity to endogenous redox changes, respectively, enabling to predict cells behavior.

Keywords

- Nanotoxicology;
- Cell death;
- Oxidative stress;
- DNA repair.

ACCEPTED MANUSCRIPT

Introduction

Titanium dioxide nanoparticles (TiO_2-NPs) are used extensively in numerous commercial products, including paint, cosmetics, plastics, paper, and food, as an anticaking or whitening agent (Wang et al., 2014). Due to their widespread use, there are increasing concerns about the biological effects of TiO_2-NPs and potential health risks for exposed workers and general population (Byrne and Baugh, 2008; Rollerova et al., 2015; Warheit and Donner, 2015). Human exposure to TiO_2-NPs may occur during both manufacturing and use. NPs are characterized by unique physico-chemical properties at the nano-scale, as well as biological properties, and the primary route of TiO_2-NPs occupational exposure is inhalation (Shi et al., 2013; Warheit and Donner, 2015). As a consequence, the understanding of NPs possible effects on the human respiratory system and particularly on air-blood barrier has become of primary interest. In this system, macrophages, lung epithelial cells and underlying endothelial cells may have a different sensitivity and behavior in response to NPs exposure. Therefore, determining the effects of inhaled particles on these cells is critical

Some studies have suggested that nanoparticles may be more toxic than larger particles of the same material because of larger surface area, enhanced chemical reactivity and easier cellular penetration (Oberdörster et al., 1992). For example, TiO_2-NPs were shown to exhibit significant toxic effects including chronic pulmonary inflammation (Shi et al., 2004). Pigment-grade titanium dioxide and ultrafine TiO_2-NPs have been studied after various routes of administration. Results from pulmonary respiratory studies provided sufficient evidence in animals for the carcinogenicity of titanium dioxide (Baan et al., 2006). The International Agency for Research on Cancer (IARC) reviewed TiO_2 data and concluded that there was sufficient evidence of carcinogenicity in experimental animals and inadequate evidence of carcinogenicity in humans (Group 2B), an overall evaluation of “possibly carcinogenic to humans”(IARC, 2010).

ACCEPTED MANUSCRIPT

The extent to which such NPs contribute to cellular toxicity may associate induction of oxidative stress pathways, leading to lung injury (Lu et al., 2014; Madl et al., 2014). Oxidative stress is the dominant hypothesis for the adverse effect of NPs at the cellular level. Reactive oxygen species (ROS) production is a normal cellular process which is involved in various aspects of cellular signaling, as well as in the defense mechanisms. However, excessive ROS production has been found to cause severe damage to cellular macromolecules such as proteins, lipids and DNA, resulting in detrimental effects on cells. Nanoparticles are known to induce ROS production, leading to an oxidative stress when redox state of the cell is imbalanced (Fahmy and Cormier, 2009; Lin et al., 2008; Manke et al., 2013a).

Publications reported that TiO_2-NPs could cause several adverse effects on mammalian cells such as increase of ROS production and cytokines levels, reduction of cell viability and proliferation, induction of apoptosis and genotoxicity (Iavicoli et al., 2011; Kansara et al., 2015). In response to DNA damage, the cells either initiate DNA repair mechanisms or trigger cell cycle arrest and apoptosis. One of the major effector molecules activated in response to DNA damage is p53. It plays a central role in DNA repair and cell cycle arrest, thereby preventing mutagenic events favoring the process of carcinogenesis (Lane, 1992). Nanoparticles-induced ROS generation has been directly implicated in genotoxicity (Falck et al., 2009; T. Chen et al., 2014; Z. Chen et al., 2014), malignant transformation and cancer (Weinberg et al., 2010). Specifically, such ROS generation has been associated with the acquisition of a tumorigenic phenotype *in vitro* and *in vivo* induced by TiO_2-NPs (Baan et al., 2006; Onuma et al., 2009; Iavicoli et al., 2011).

Moreover, both *in vitro* and *in vivo* studies showed that nanoparticles-induced lung injury and pulmonary fibrosis may be linked to the ROS production (Byrne and Baugh, 2008). Such stress response may involved signaling such as the MAPK pathway that regulates a diverse range of cellular responses, including cell proliferation, differentiation, mitosis, cell survival and apoptosis. They are a family of serine/threonine protein kinases that include growth

ACCEPTED MANUSCRIPT

factor-regulated extracellular signal-related kinases (ERK) and the stress-activated MAPK, c-Jun NH2-terminal kinases (JNK) and P38 MAPK. The ERKs are mainly associated with cell proliferation and differentiation, whereas the JNKs and p38 MAPKs are known to regulate responses to cellular stresses. The P38 MAPK and/or ERK pathway was suggested to mediate toxicity in human bronchial epithelial cell line upon treatment with titanium dioxide nanoparticles (Park et al., 2008).

Although the link between ROS, damage and lung injury are increasingly discussed today (Lu et al., 2014; Madl et al., 2014), few data are available concerning the predictability of response of cellular models. The exact cascade of signaling molecules mediating ROS generation and apoptosis in nanoparticle-induced toxicity is poorly studied (Huang Yue-Wern, 2010), and thus attempts to better understand this mechanism may prove useful in reducing the toxicological side effects. More studies are required to elucidate toxicity pathways, the oxidative stress effects and the response mechanisms triggered by this material, which would allow the identification of potential biomarkers.

In this context, to further understand the toxicological behavior of TiO_2-NPs and the underlying mechanisms, we evaluated the cytotoxic effect of TiO2-NPs using model cell lines constitutive of the alveolo-capillary barrier, i.e. the alveolar macrophage-like THP-1, alveolar epithelial A549 and Human Pulmonary Microvascular Endothelial Cells HPMEC-ST1.6R cells. Cell lines are representative of our target organ (lung), and were chosen because of their prevalence in the literature. These are robust models, widely used and described in the context of nanotoxicology (Foster et al., 1998; Chanput et al., 2014; Mirowsky et al., 2015).

To address oxidative stress responses, we investigated the impact of modulation of endogenous glutathione (GSH) content by using a depletion or supplementation balance on ROS generation and consequences on cytotoxicity. GSH is the major ROS-scavenging system in cells and the important redox modulating enzymes including the peroxidases, peroxiredoxins and thiol reductases rely on the pool of reduced GSH in the cell as their

ACCEPTED MANUSCRIPT

source of reducing equivalents (Forman et al., 2009). Therefore, strategies to induce a loss of reduced GSH pool are expected to have a major effect on cell survival and sensitivity to nanoparticles exposition by altering the ability of cells to detoxify ROS and therefore by triggering cell death. This can be achieved by targeting its synthesis with buthionine sulfoximine (BSO), an inhibitor of glutamylcysteine ligase (γ-GCL), the rate-limiting enzyme for GSH synthesis. Previous reports have presented evidence for the effectiveness of BSO in sensitizing cell lines in combination with other drugs (Leung et al., 1993; Buchmüller-Rouiller et al., 1995; Lewis-Wambi et al., 2009; Lee et al., 2010). BSO is used combined with dimethylfumarate (DMF), to deplete cell in their glutathione content (Albrecht et al., 2012; Hanot et al., 2012). On another hand, N-acetyl-cysteine (NAC) is a quite popular antioxidant used for their ability to minimize oxidative stress and the downstream negative effects thought to be associated with oxidative stress. NAC is a by-product of glutathione and is popular due to its cysteine residues and the role it has on glutathione maintenance and metabolism (Kerksick and Willoughby, 2005; Forman et al., 2009). Nac is used to supplement cells in thiol functions.

In order to achieve a representative response of local lung toxicology, exposures were performed using a wide range of nanoparticles concentrations (from 5 to 800 µg/ml, corresponding to 1 to 160 µg/cm^2). Lower doses represented environmental exposure, while higher one considered the possibility of a pulmonary local hot spot distribution of nanoparticles (Donaldson and Poland, 2012; Qiao et al., 2015; Veranth et al., 2010).

The genotoxic potential of TiO_2-NPs was investigated using the activation of γH2AX, and evaluation of different types of DNA repair proteins and cell cycle arrest. Furthermore, in an attempt to determine potential biomarkers predictive of cell death or cell behavior, stress-activated protein kinases were also investigated for a 24h exposure to TiO_2-NPs.

ACCEPTED MANUSCRIPT

Materials and Methods

Chemicals

All antibodies were purchased from Cell Signaling Technology® (DNA Damage Antibody Sampler Kit #9947 and Stress and Apoptosis Antibody Sampler Kit #8357).TiO_2-NPs from AEROXIDE® TiO_2 P 25, were purchased from Evonik Industries.

Cell lines and culture medium

A549 (ATCC number: CCL-185™) and THP-1 (ATCC number: TIB-202™) cell lines were obtained from LGC Standards. They were routinely grown in RPMI 1640 medium supplemented with 10% (v/v) heat-inactivated foetal bovine serum (Sigma- Aldrich), 1% (v/v) Penicillin/Streptomycin (Invitrogen). THP-1 cells (non-adherent monocytic cells) were routinely maintained at undifferentiated state. For experiments, they were differentiated in macrophage-like adherent cells using a 24 h incubation with 30 ng/mL of PMA (Phorbol 12-myristate 13-acetate; Sigma-Aldrich), according to the method described by Lanone et al. (Lanone et al., 2009). The Institute of Pathology of Mainz in Germany kindly provided Human Pulmonary Microvascular Endothelial Cells (HPMEC-ST1.6R). These cells were routinely maintained on tissue culture plastic ware pre-coated with gelatin (BD Biosciences) in M199 medium (Sigma-Aldrich) supplemented with 20% (v/v) heat-inactivated FCS, 50 µg/mL endothelial cell growth supplements (Sigma-Aldrich), 25 µg/mL sodium heparin (Sigma-Aldrich) and 1%(v/v) Penicillin/Streptomycin (Krump-Konvalinkova et al., 2001).

Glutathione depletion or supplementation pre-treatment

A transient glutathione-depletion strategy was applied before exposition to NPs, based on the use of dimethylfumarate (DMF), a glutathione-depleting agent, and buthionine sulfoximine (BSO), a glutathione biosynthesis inhibitor. DMF (100 mM) and BSO (100 mM) were both added to the cell culture medium for 4 h to deplete glutathione, as described previously on cells having a very high glutathione content (Boivin et al., 2011; Hanot et al.,

ACCEPTED MANUSCRIPT

2012). Such pre-treatment was named DMF/BSO pre-treatment. Cell cultures were washed twice with fresh culture medium before exposition to NPs.

In order to supplement cells with molecules carrying a thiol function in order to overcrowded cells in ROS scavenger, N-acetyl cysteine (NAC, 5 mM) was also added to the culture medium 4 h, then cell cultures were washed twice before NPs exposition.

Intracellular generation of ROS

Cells were seeded on a 24 well plate (5.10^5 THP-1 cells, 6. 10^4 A549 cells or $1{,}5.10^4$ HPMEC-ST1.6R cells per well) and incubated at 37°C, 4% CO_2 for 24 h. Cells were exposed to NPs (5, 200 and 800 µg/ml concentrations, corresponding to 1, 40, 160 µg/cm^2) in complete medium for 4 h and 24 h. CM-H2DCFDA (General Oxidative Stress Indicator, C6827, Molecular probes^{TM}) probe is air, light and temperature sensitive so great care was taken when preparing 10 mM CM-H2DCFDA stock solution made in dimethyl sulfoxide (DMSO) and then diluted warm PBS to yield a 10 µM working solution. Following nanoparticles exposure, cells were rinsed with PBS and 500 µL of DCFH-DA working solution (10 µM in warm PBS) was added before the plates were incubated in the dark at 37°C for 30 min. Cells were rinsed with pre-warmed PBS and 200 µl of 90% DMSO in PBS was added and incubated for 5 min at 37°C. The plates were protected from light before being centrifuged for 5 min at 250 g. Measurement of 150 µl of supernatant was performed in black 96 well plates at an excitation wavelength of 488 nm and emission wavelength of 530 nm.

Dispersion and characterization of TiO_2-NPs

TiO_2-NPs were suspended at a concentration of 10 mg/mL in RPMI 1640 culture media without phenol red (Invitrogen) supplemented with 5% (v/v) heat-inactivated foetal bovine serum (Sigma- Aldrich), 1% (v/v) Penicillin/Streptomycin. Suspensions were sonicated

ACCEPTED MANUSCRIPT

10 min (1 min pause every 1 min) at 60 W with a cuphorn (Sonicator S-4000, Misonix incorporated), while avoiding contamination by the probe. During sonication, the dispersions were maintained at temperature with an ice/water bath to prevent heating. The size, polydispersity index (PDI), and zeta potential of the suspension were characterized by Dynamic Light Scattering (DLS) using a Zetasizer Nano ZS (Malvern Instrument, Westborough, MA). The dispersions were also characterized by transmission electron microscopy (TEM) using a few drops of the material dispersed in double-distilled water on a carbon/ formvar-coated grid and allowed to air dry.

Cell viability assay

Cell viability was measured by the CellTiter 96® AQueous One Solution Cell Proliferation Assay. Solution Reagent contains a novel tetrazolium compound [3-(4,5-dimethylthiazol-2-yl)-5-(3-carboxymethoxyphenyl)-2-(4-sulfophenyl)-2H-tetrazolium, MTS]. Cells were seeded on 96-well culture plates with 8.10^4 THP-1 cells, 1.10^4 A549 cells and 3.10^4 HPMEC-ST1.6R cells in 100 µl media per well. After a 24 h stabilization, cells were exposed to a freshly prepared TiO_2-NPs suspension in cell media (5, 25, 50, 100, 200, 400 and 800 µg/ml concentrations, corresponding to 1, 5, 10, 20, 40, 160 µg/cm^2) for 24 h. At the end of exposure, cells were washed twice with fresh and pre-warmed media in order to eliminate a maximum of nanoparticles and avoid interaction with the colorant. The cells were incubated for 1-2 h at 37°C with 80 µl media per well supplemented with 20 µl of CellTiter 96® AQueous One Solution Reagent. Plates were centrifuged for 10 min at 2000 rpm and supernatant collected for measurements. The absorbance was measured at 490 nm using a microplate spectrophotometer system (TECAN Infinite M2000, Switzerland). The viability of the treated cells was expressed as a percentage of non-treated control cells, which was assumed to be 100%.

ACCEPTED MANUSCRIPT

Cellular apoptosis/necrosis assay.

Apoptosis was assessed with the Annexin V-FITC kit according to the manufacturer's instructions (BioVision, Milpitas, CA, USA). Dual staining with fluorescent Annexin V and propidium iodide (PI) has been used to discriminate apoptotic and necrotic cell death, in which Annexin V-positive/PI-negative staining is regarded as apoptosis and PI-positive staining as necrosis Cells were seeded on 25 cm^2 culture plates with $6.2.10^6$ THP-1 cells, $0.8.10^6$ A549 cells and $2.5.10^6$ HPMEC-ST1.6R cells in 5 ml media per plate. After a 24 h stabilization, cells were exposed to a freshly prepared TiO_2-NPs suspension in cell media (5, 200 and 800 µg/ml concentrations, corresponding to 1, 40, 160 µg/cm^2) for 24 h. Cells were washed twice with cold PBS, collected, and resuspended in binding buffer. Annexin V-FITC and propidium iodide were added, and the cells were incubated for 10 min at room temperature in the dark. The cells were calculated with flow cytometry (CyanTM ADP flow cytometer, Beckman Coulter).

Cell cycle assay.

Cells were seeded on 25 cm^2 culture plates and exposed to a freshly prepared TiO_2-NPs suspension in cell media (5, 200 and 800 µg/ml concentrations, corresponding to 1, 40, 160 µg/cm^2). Cells pellets were digested and collected by trypsin, fixed in 70% ethanol on ice and then stained with 5 µg/ml propidium iodide (PI) (Sigma, St. Louis, MO, USA) and 0,1 µg/ml RNase A (Sigma). The cells were detected with Epics XL-MCL flow cytometer (Beckman Coulter). Cell Quest software (BD CellQuest Pro Software, BD Biosciences, San Diego, CA, USA) was used to analyze the percentage of the cell population in each phase.

Western blot analysis.

Cells were seeded on 25 cm^2 culture plates and exposed to a freshly prepared TiO_2-NPs suspension in cell media (5, 200 and 800 µg/ml concentrations, corresponding to 1, 40, 160 µg/cm^2). Total cell proteins were extracted with cell lysis buffer (150 mM NaCl, 50 mM Tris (pH 8), 1% Triton X-100 and protease and phosphatases inhibitors), then, lysates were

ACCEPTED MANUSCRIPT

centrifuged for 20 min at 15.000 g. Protein content was determined using the BCA protein assay kit (Thermo Scientific Pierce, # 23225). Forty milligrams of total proteins were loaded and separated on 12 % SDS-PAGE gels, and transferred onto nitrocellulose membranes (Millipore, Billerica, MA, USA). Membranes were cut in 4 parts, depending on the size of the observed proteins, incubated with. the primary antibodies (1:1.000) at 4˚C overnight, and bound with HRP-conjugated secondary antibodies at room temperature for 1 h. Chemiluminescent signaling was detected using an ECL kit (Millipore). When necessary, a stripping of membranes (stripping solution: 25 mM Glycine-HCl, pH2, 1% (w/v) SDS) was performed to entirely remove the fixed antibody and allow incubation with a different primary antibody. Semi-quantitative analyses of western blot were performed using Gel Analysis plugging of ImageJ free software (http://rsb.info.nih.gov/ij/index.html). Ratio of proteins were represented relatively to GAPDH production.

Statistical analysis

Data from at least three independent experiments are presented as the mean and standard deviation. Statistical analysis were performed with GrapPad software, using two-way analysis of variance (ANOVA) followed by Bonferroni post-test. NPs treated samples were compared with their respective controls. DMF/BSO pre-treated groups and NAC pre-treated groups were compared with their respective NPs treated samples without pre-treatment. $P<0.05$ was considered significant.

Results

Physical and chemical characterization of test TiO_2-NPs

Differences in particle size, dispersion or agglomeration have been shown to play an important role in nanoparticle interaction with cell membranes and toxicity. We therefore, determined selected physical properties of the particles in the physiological media containing the culture media and serum. Data indicated that nano-sized particles had large agglomerate sizes (DLS measurements) in solution (mean agglomerate size was 400 nm). Size and

ACCEPTED MANUSCRIPT

shape of particles were also assessed using transmission electron microscopy (TEM) (Fig. 1). The particles were mostly dispersed as agglomerates or aggregates. However, all dispersions also contained nanosized particles as verified by TEM analysis. Stability of suspension evaluated with potential zeta was –12 mV. The polydispersity index value was 0.5 for TiO_2-NPs, revealing this sample had a very broad size distribution and may have contained large aggregates that could slowly sediment. Visually, sedimentation occurred during the exposure.

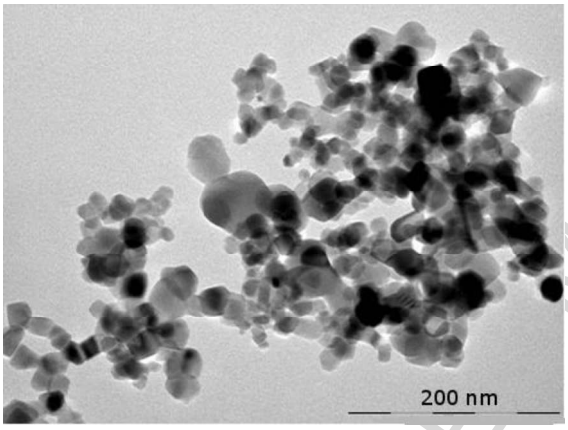


Fig. 1.tiff: single column fitting image

Characterization of TiO_2 particles by transmission electron microscopy (TEM). All dispersions contained nanosized particles; however the particles were mostly dispersed as agglomerates or aggregates.

Measurement of intracellular ROS

To investigate whether TiO_2-NPs could trigger ROS generation, the intracellular ROS level was measured using CM-H_2DCFDA probe, 4 h and 24 h after NPs treatment at 5, 200 and 800 µg/ml (Fig. 2). Experimental conditions using NAC or DMF/BSO pre-treatment were also investigated to assess the role of glutathione and endogenous protection of cell lines.

In THP-1 cells, an increase of fluorescence signal corresponding to a significant concentration-dependent increase in % of ROS generation was observed, only 24 h after treatment with TiO_2-NPs (182,5% ±14,8 and 266,3% ±16,4 at 200 and 800 µg/ml respectively). In this case, a pre-treatment with NAC led to the suppression of ROS

ACCEPTED MANUSCRIPT

generation observed 24 h after NPs treatment, while a DMF/BSO pre-treatment led to a significant increase of ROS generation (260,1% ±12,9 and 365,4% ±16,6 at 200 and 800 µg/ml respectively).

For A549 and HPMEC-ST1.6R cell lines, a dose-dependent increase in % of ROS generation was also observed, but the time course was different, with a maximal increase observed as early as 4 h after NPs incubation. ROS generation reached a maximum of 339,5% ±12,2 in A549 cells and 306,6% ±14,1 in HPMEC-ST1.6R cells at 800 µg/ml of NPs.

For both A549 and HPMEC-ST1.6R cell lines, NAC pre-treatment led to a weak ROS generation 4 h after treatment with the higher NPs dose (237,9% ±33,8 for A549 and 226,5% ±22,4 for HPMEC-ST1.6R cells), while DMF/BSO pre-treatment increased it (383,2% ±7,8 for A549 and 354,2% ±21,1 for HPMEC-ST1.6R cells).

After 24 h of NPs exposure, a slight but significant ROS generation increase was observed for A549 and HPMEC-ST1.6R, for higher doses only (did not exceed 200% of ROS generation at the highest concentration). At this time point, pre-treatment using NAC or DMF/BSO did not impact ROS generation in A549 cells. For HPMEC-ST1.6R cells, only DMF/BSO pre-treatment led to a significant but slight modification of ROS generation at 200 and 800 µg/ml (148,6% ±8,6 and 123,7% ±3,9, respectively).

DMF/BSO pre-treatment induced an increase of generated intracellular oxidative stress, while NAC supplementation, decreased it.

ACCEPTED MANUSCRIPT

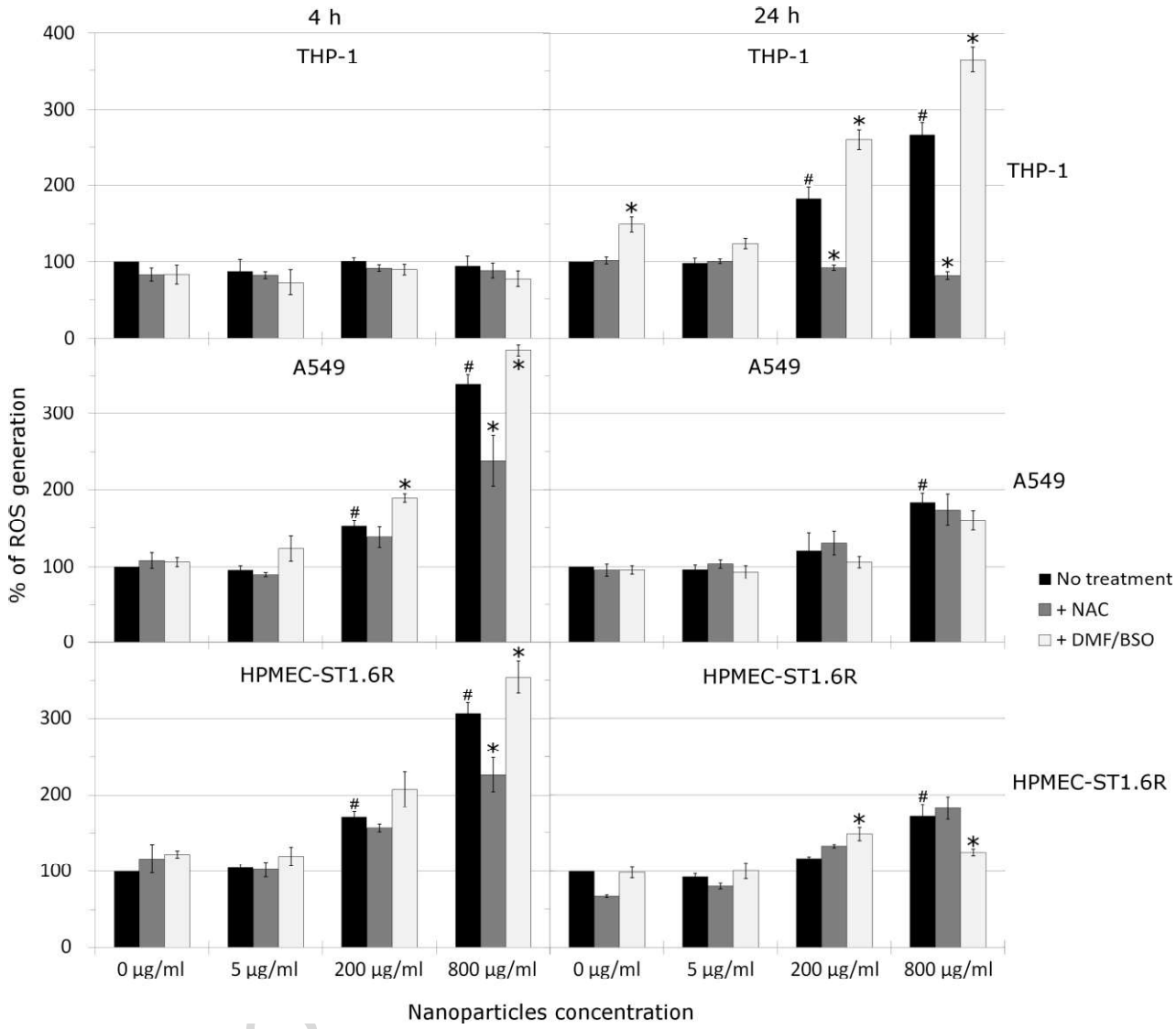


Fig. 2.tiff: 2- column fitting image

Production of ROS detected with CM-H_2DCFDA probe. Percentage of ROS generation was calculated compared to the untreated control cells. Black bar showed TiO_2-NPs treated group, grey bar showed DMF/BSO/TiO_2 treated group and white bar showed NAC/TiO_2 treated group. # indicates that TiO_2-NPs treated group is statistically significant from untreated group ($p < 0.05$) and ✱ indicates that DMF/BSO/TiO_2 treated group is statistically significant from the TiO_2-NPs treated group ($p < 0.05$). DMF/BSO pre-treatment induced an increase of generated intracellular oxidative stress, while NAC supplementation, decreased it.

ACCEPTED MANUSCRIPT

Cytotoxicity of TiO_2-NPs

TiO_2-NPs effects on cell viability were examined after 24 h exposure, using the MTS assay (Fig. 3). Cells lines were incubated with gradually increasing concentrations (0 to 800 µg/ml) of TiO_2-NPs. Part of experiment were conducted with or without N-acetyl-cysteine (NAC) to supplement cells in thiol molecule functions, and with or without DMF/BSO pre-treatment to deplete cells in endogenous glutathione content and inhibit its synthesis.

A statistically significant cytotoxic effect of TiO_2-NPs was observed on micro-vascular cells (HPMEC-ST1.6R), starting at 50 µg/ml and observed in a dose-dependent manner (Fig. 3C). In contrast, no significant cytotoxicity was observed in macrophages (differentiated THP-1) and epithelial cells (A549),.

In experiments with NAC addition, no significant modification viability was observed compared to exposition with TiO_2-NPs alone, in any cell lines tested. However, with DMF/BSO pre-treatment, THP-1 and HPMEC-ST1.6R cell lines displayed a significant cell death increase starting at 25 µg/ml of TiO_2-NPs. Cell viability decreased in a dose dependant manner to reach 67,8% ±5,5 for THP-1 and 60,3% ±4,9 for HPMEC-ST1.6R cell lines. No significant modification in A549 cell viability was observed with DMF/BSO pre-treatment.

THP-1 and HPMEC-ST1.6R cell lines were sensitive to redox state modulation induced by DMF/BSO pre-treatment.

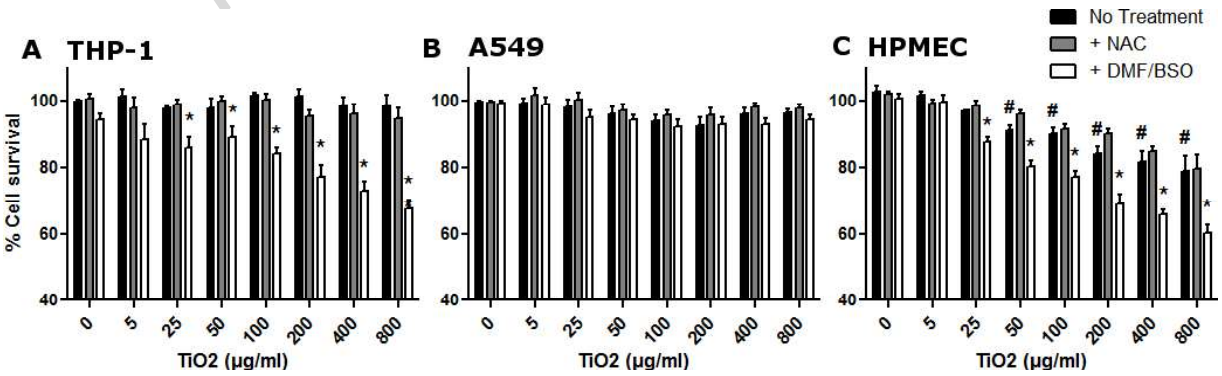


Fig.3.tiff: 2- column fitting image

ACCEPTED MANUSCRIPT

Effects of TiO_2 particles on cells viability after 24 h. Cell viability was assessed by the MTS assay, and results are presented as a percentage of control group viability. Black bar correspond to TiO_2-NPs treated group, grey bar to DMF/BSO/TiO_2 treated group and white bar to NAC/TiO_2 treated group. Data are expressed as the mean ± SD of at least three independent experiments; # indicated that TiO_2-NPs treated group is statistically significant from their respective untreated controls ($p < 0.05$). * indicatesd that DMF/BSO/TiO_2 treated group is statistically significant from their respective TiO_2-NPs treated group ($p < 0.05$). THP-1 and HPMEC-ST1.6R cell lines were sensitive to redox state modulation induced by DMF/BSO pre-treatment.

Apoptosis/necrosis analysis by flow cytometry

To adresse the cell death type induced by NPs, the percentage of cells undergoing apoptosis and necrosis was examined quantitatively by flow cytometry (Table 1). Annexin V/PI staining combined with flow cytometry is used to differentiate between viable and dead cells (as a result of either apoptosis or necrosis). Results showed that no necrosis induction happened after TiO_2 exposition, whatever the combined pre-treatment used (table 1B).

THP-1 cell line underwent apoptosis only when exposed to TiO_2-NPs combined with DMF/BSO pre-treatment (table 1A). No significative percentage of apoptosis was observed in A549 cells. HPMEC-ST1.6R displayed a dose-dependent increase of apoptotic cells when exposed to TiO_2-NPs. Pre-treatment with DMF/BSO increased apoptosis induction in HPMEC-ST1.6R cell line when compared to exposition with TiO_2-NPs only, the maximum reaching 41,0% ±3,4 at 800 µg/ml. A combined exposure with NAC gave similar cell death induction as exposure with TiO_2-NPs only, in all three cell lines.

Apoptosis was the major cell death induced, and quantification of apoptotic cell death gave similar results to those observed with MTS assays.

ACCEPTED MANUSCRIPT

A

% Apoptotic cells ± SD

	[NPs] µg/ml	∅	+ NAC	+ DMF/BSO
THP-1	0	2,2 ± 3,7	1,2 ± 1,1	5,0 ± 3,7
	5	4,5 ± 3,9	3,2 ± 5,3	**14,0 ± 4,4**[a b]
	200	4,9 ± 3,5	5,3 ± 4,3	**20,2 ± 5,1**[a b]
	800	6,3 ± 3,7	4,4 ± 3,9	**33,9 ± 5,9**[a b]
A549	0	2,3 ± 1,8	0,1 ± 0,0	1,5 ± 2,0
	5	2,6 ± 2,3	0,6 ± 0,8	2,6 ± 0,8
	200	2,9 ± 0,6	1,3 ± 1,8	3,6 ± 0,6
	800	5,3 ± 3,1	3,1 ± 1,6	2,9 ± 0,7
HPMEC	0	2,0 ± 2,5	1,5 ± 0,7	3,2 ± 0,8
	5	**9,3 ± 2,5**[a]	5,5 ± 0,8[a]	**19,5 ± 0,8**[a b]
	200	**13,7 ± 1,4**[a]	13,8 ± 1,6[a]	**24,9 ± 5,2**[a b]
	800	**19,8 ± 3,4**[a]	15,5 ± 2,4[a]	**41,0 ± 3,4**[a b]

B

% Necrotic cells ± SD

	[NPs] µg/ml	∅	+ NAC	+ DMF/BSO
THP-1	0	0,1 ± 0,0	0,2 ± 0,2	1,1 ± 1,0
	5	2,1 ± 1,2	1,1 ± 1,3	1,3 ± 1,1
	200	2,9 ± 1,2	3,7 ± 2,2	3,0 ± 1,1
	800	2,0 ± 2,0	1,5 ± 1,2	4,9 ± 3,4
A549	0	0,8 ± 0,5	0,8 ± 0,1	1,1 ± 0,5
	5	1,5 ± 1,3	0,0 ± 0,0	1,3 ± 1,6
	200	2,1 ± 0,9	2,9 ± 0,4	3,0 ± 1,5
	800	1,3 ± 1,6	4,2 ± 1,5	4,9 ± 1,8
HPMEC	0	2,7 ± 1,1	0,9 ± 0,5	3,1 ± 0,7
	5	2,2 ± 1,7	2,0 ± 2,9	3,0 ± 0,8
	200	2,1 ± 1,0	2,7 ± 0,3	3,3 ± 1,0
	800	2,9 ± 1,6	3,3 ± 0,8	4,6 ± 0,5

Table 1.tiff: 2- column fitting image

Apoptosis/necrosis analysis by flow cytometry. Summary of the percentage of cells undergoing apoptosis (A) and necrosis (B) expressed as mean ± SD of at least three independent experiments. ∅, +DMF/BSO, +NAC indicated no pre-treatment applied, pre-treatment with DMF/BSO and pre-treatment with NAC, respectively;. [a] indicated that samples treated with TiO_2-NPs were significantly different from their respective control at 0 mg/ml of nanoparticles ($p < 0.05$). [b] indicated that samples pre-treated with DMF/BSO were significantly different from their respective samples group without pre-treatment ∅ ($p < 0.05$). Major cell death mechanism involved apoptosis.

Effects of TiO_2 on cell cycle

Cell cycle checkpoints are control mechanisms that ensure the fidelity of cell division. These checkpoints verify whether the processes at each phase of the cell cycle have been accurately completed before progression into the next phase. Cell cycle analyses were performed on A549 and HPMEC-ST1.6R cells by flow cytometry. Differentiated THP-1 macrophages, which are non-cycling cells, were not investigated.

Results are presented in figure 4. For A549 cells, at all TiO_2-NPs concentrations tested, a 24 h exposure did not induce any cell accumulation in a cell cycle phase, so cell cycle progression was not impacted by TiO2-NPs exposure. In contrast, HPMEC-ST1.6R cells

ACCEPTED MANUSCRIPT

displayed an accumulation of cells in the S phase of the cycle. The blocking in S phase appeared dose-dependent and was significant already at the lowest dose (48,8% ±2,4 at 5 µg/ml). This accumulation was concomitant with the loss of a proportion of cells engaged in the G2 phase, down to 4,2% ±3,5 for the highest concentration.

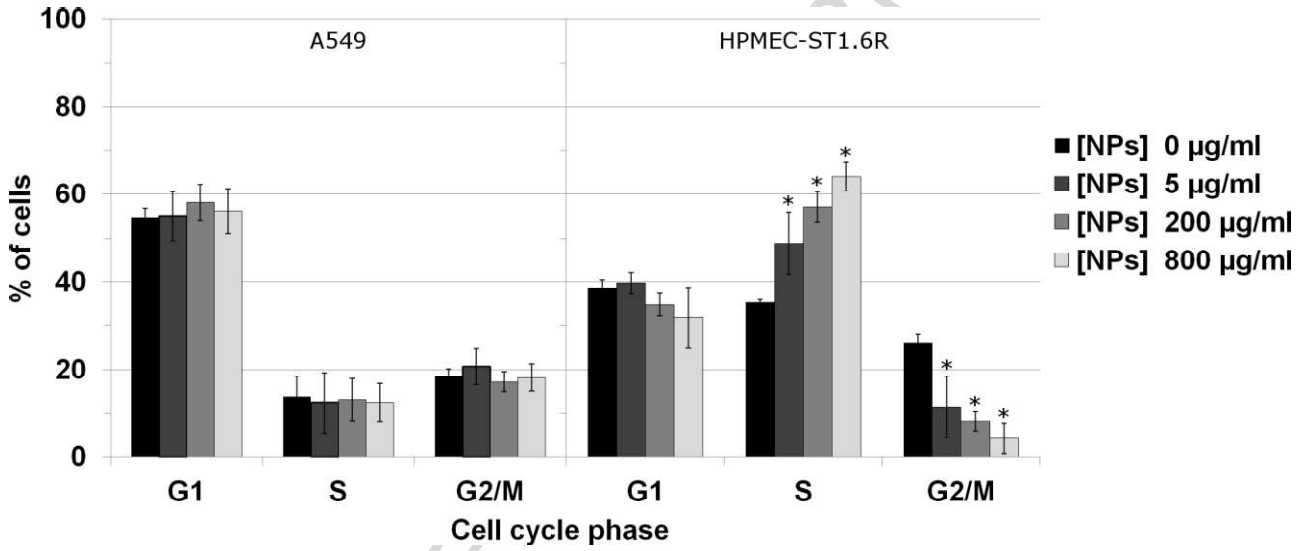


Fig. 4.tiff: 2- column fitting image

Cell cycle phase distribution. A549 and HPMEC-ST1.6R cell cycle phase were observed after a 24 h TiO_2-NPs exposure. * indicates that results for the TiO_2-NPs treated group is significantly different ($p < 0.05$) from untreated group. Therefore, our results show that HPMEC-ST1.6R cells displayed a dose-dependent accumulation in the S phase of cell cycle in response to TiO2 exposure, but not A549 cells.

Major signaling checkpoints in response to DNA damage by Western blot analysis

To further assess and analyze major signaling checkpoints in response to DNA damage, western blot analyses were performed. Ataxia telangiectasia mutated kinase (ATM) and ataxia telangiectasia and Rad3-related kinase (ATR) are PI3 Kinase-related kinase family members that phosphorylate multiple substrates on serine or threonine residues that are followed by a glutamine in response to DNA damage or replication blocks (Abraham, 2004;

ACCEPTED MANUSCRIPT

Shechter et al., 2004). P53 is phosphorylated by ATM, ATR and DNA-PK at Ser15. This phosphorylation impairs the ability of MDM2 to bind P53, promoting both the accumulation and activation of P53 in response to DNA damage (Shieh et al., 1997; Martinho et al., 1998). Chk1 and Chk2, downstream protein kinases of ATM/ATR, play an important role in DNA damage checkpoint control (Yan et al., 2014). Chk1 and Chk2 are phosphorylated following DNA damage by ATM/ATR (Ahn et al., 2000; Matsuoka et al., 2000). The breast cancer susceptibility proteins BRCA1 and BRCA2 are frequently mutated in cases of hereditary breast and ovarian cancers and have roles in multiple processes related to DNA damage, repair, cell cycle progression, transcription, ubiquitination and apoptosis. Numerous DNA-damage induced phosphorylation on BRCA1 and kinases activated in a cell cycle-dependent manner. DNA damage also induces rapid phosphorylation of the histone H2A family member H2AX by ATM (Rogakou et al., 1998; Pouliliou and Koukourakis, 2014). Within minutes following DNA damage, γH2AX localizes to sites of DNA damage at subnuclear foci.

Cell lines displayed different activated pathways 24 h after NPs exposure (Fig. 5 and 6). In differentiated THP-1 macrophages, phosphorylation of ATR increased with increasing concentrations of TiO_2-NPs, from 200 to 800 µg/ml. A clear concomitant phosphorylation of ATM was observable at 200 and 800 µg/ml. Remarkably, phosphorylation of H2AX histone (γH2AX) was also observed, for the same concentrations, revealing the high persistence of deleterious DNA lesions and downstream activation of pathway.

In HPMEC-ST1.6R cells, phosphorylation of H2AX histone was observed, with no activation of ATR or ATM proteins. Otherwise, P53 and checkpoint protein ChK1 phosphorylation occurred at 200 and 800 µg/ml, correlating with a cell cycle arrest.

No activation of signaling pathways related to DNA damage was observed in A549 cell line 24h post-treatment. All together, these results showed that, in the same conditions of exposure, the three cell lines exhibited different profiles of activated signaling in response to DNA damage.

ACCEPTED MANUSCRIPT

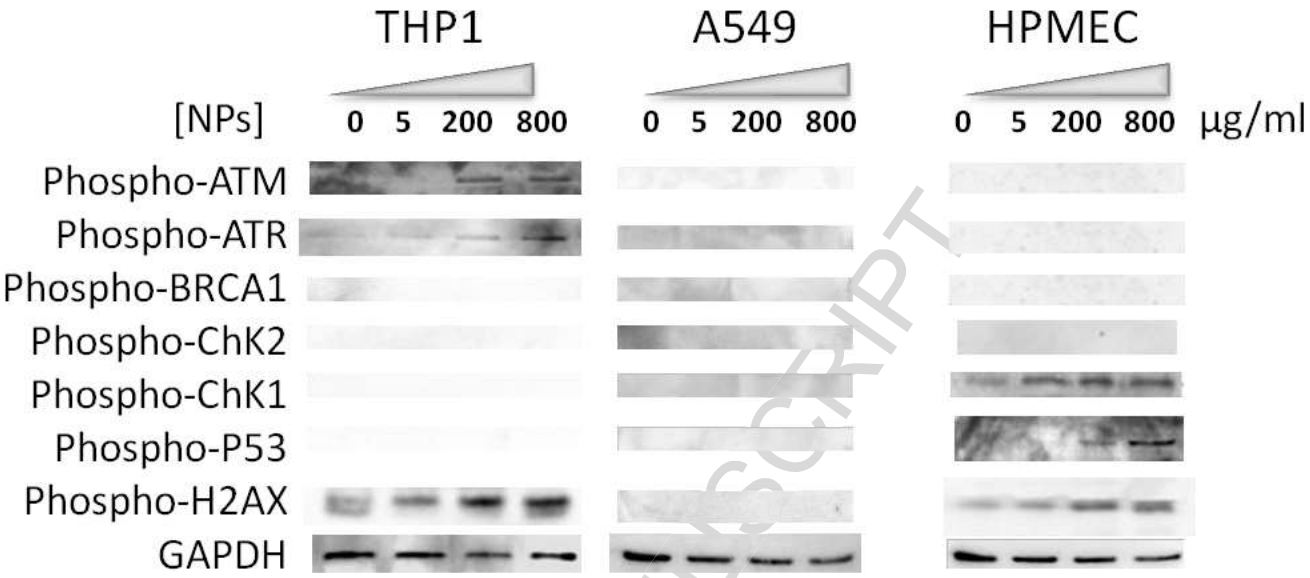


Fig. 5.tiff: 2- column fitting image

Representative Western blots of major signaling checkpoints in response to DNA damage. Cell lines were treated with TiO_2-NPs for 24h in three different concentrations.

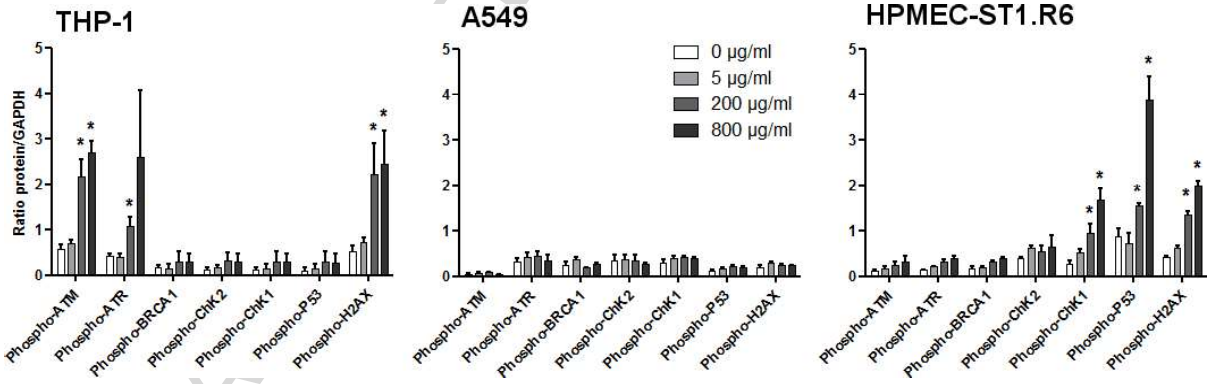


Fig 6.tiff: 2- column fitting image

Semi-quantification of protein activation related to DNA repair. Ratios of proteins were represented relatively to GAPDH production (mean ±SD). * indicates that TiO_2-NPs treated group is significantly different ($p < 0.05$) from their respective controls. THP-1 and HPMEC cell lines displayed activation of protein related to DNA repair.

Western blot analysis of stress and apoptotic signaling

Cells respond to environmental or intracellular stresses through various mechanisms ranging from initiation of pro-survival strategies to activation of cell death pathways leading to

ACCEPTED MANUSCRIPT

removal of damaged cells from the organism. Many of the proteins and cellular processes involved in normal signaling and survival pathways also play a role in cell death-promoting mechanisms.

To evaluate effects of TiO_2 on stress and apoptosis signaling, we determined expression profiles of key proteins in apoptosis pathways and in the MAP and SAPK/JNK kinases pathways (Fig. 7 and 8).

Apoptosis signaling may be assessed by cleavage of caspase-3 and nuclear poly (ADP-ribose) polymerase (PARP) proteins. Caspase-3 plays a critical role in apoptosis, as it is either partially or totally responsible for the proteolytic cleavage of many key proteins, such as the nuclear enzyme poly (ADP-ribose) polymerase (PARP). Activation of caspase-3 requires its proteolytic processing in cleaved-caspase-3. PARP is involved in DNA repair in response to environmental stress. PARP helps cells to maintain their viability; cleavage of PARP facilitates cellular disassembly and serves as a marker of cells undergoing apoptosis. Results presented in Fig. 6 showed that both cleaved proteins were observed in response to NPs exposition in HPMEC-ST1.6R cell line, but not in A549 and THP-1 cell lines (Fig. 8). Such observation is concordant with cytotoxicity measurements.

P38 MAP kinase participates in a signaling cascade controlling cellular responses to cytokines and stress. MAPKAPK2 and HSP27 are downstream effectors of p38 MAP kinase. Theses kinases are involved in many cellular processes including stress, inflammatory responses, and cell death control. HSP27 may induce glutathione resynthesis in response to oxidative stress to protect cells against oxidative burst. Here, the three cell lines displayed different profiles of activated proteins after exposure to TiO_2-NPs (Fig 6). In HPMEC-ST1.6R cell line, P38 and MAPKAPK2 seemed phosphorylated on protein spot bands however, semi-quantification analysis was not significative (Fig. 8). On anoter hand, downstream effector HSP27 is witch on for all concentrations of NPs (Fig. 8).. In A549 cells, P38 and its downstream effector HSP27 were activated. In THP-1 cells, only HSP27 was significantly

ACCEPTED MANUSCRIPT

activated (Fig. 8). We noted that HSP27 was activated in the three cell lines when exposed to NPs at all concentrations tested.

The stress-activated protein kinase/Jun-amino-terminal kinase SAPK/JNK is preferentially activated by a variety of environmental stresses, and when active as a dimer, can translocate to the nucleus and regulate transcription through its effects on c-Jun, involved in regulation of genes exerting diverse biological functions including cell proliferation, differentiation, and apoptosis. SAPK/JNK and C-jun pathways were activated at medium and higher concentrations tested in HPMEC-ST1.6R and THP-1 cell lines, but not in A549 (Fig. 8), after a 24 h exposure to TiO_2-NPs.

Activation of HSP27 appeared as a common marker.

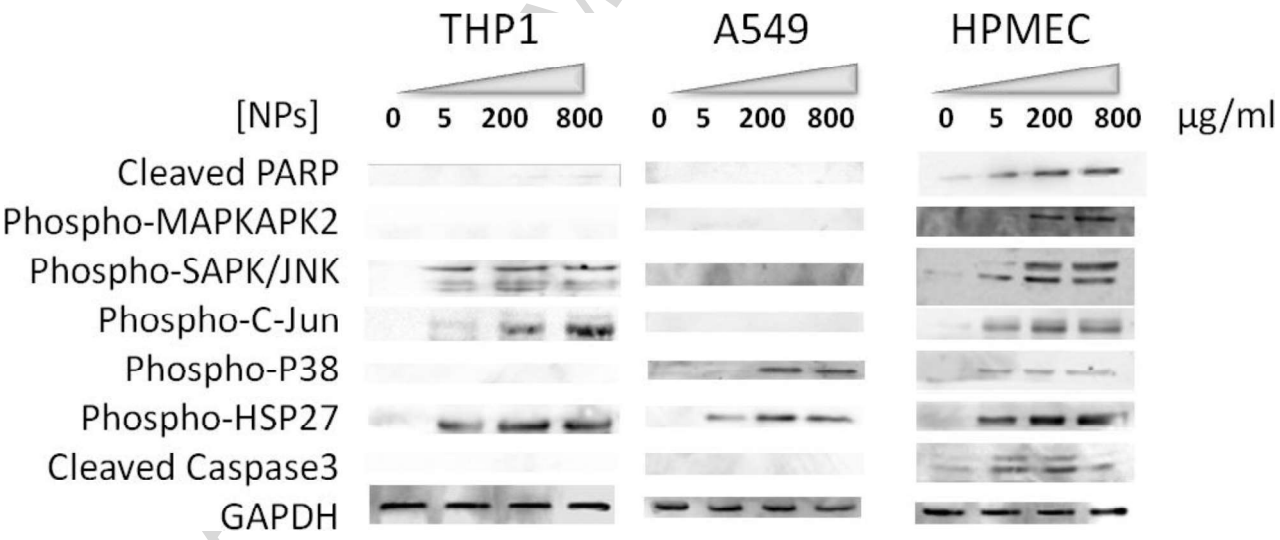


Fig.7.tiff: 2- column fitting image

Representative Western blots of stress and apoptotic signaling. Cell lines were treated with TiO_2-NPs for 24h in three different concentrations. Activation of HSP27 appeared as a common marker.

ACCEPTED MANUSCRIPT

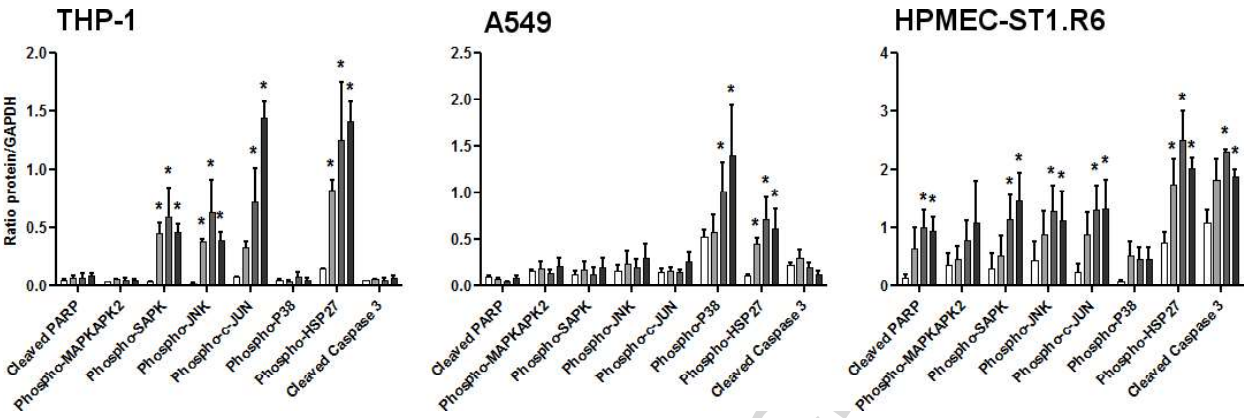


Fig 8.tiff: 2- column fitting image

Semi-quantification of protein activation related to oxidative stress. Ratios of proteins were represented relatively to GAPDH production (mean ±SD). * indicates that TiO_2-NPs treated group is significantly different ($p < 0.05$) from respective controls. Activation of HSP27 appeared as a common marker.

Discussion

During the last decades the application of nano-objects to daily-life goods and the emissions produced in highly urbanized cities have considerably increased. As a consequence, the understanding of the possible effects of NPs on human respiratory system and particularly on cells constituting the air-blood barrier has become of primary interest to explore the local toxicity. In this study, we studied oxidative stress impact on cytotoxicity and genotoxicity, in three cell lines, representative of the cell types (epithelial, endothelial and macrophages) found in the air-blood barrier in vivo, after exposure to TiO_2 NPs in the same exposure conditions. Cells were exposed to a wide range of nanoparticles concentrations; lower doses represented environmental exposure, while higher one considered the possibility of a pulmonary local hot spot distribution of nanoparticles.

Various endpoints were assessed after a 24 h exposition to TiO_2-NPs. To explore the impact of oxidative stress in cell response exposed to NPs, a combined treatment with NAC, which

ACCEPTED MANUSCRIPT

supplements cells in thiol molecule functions, or glutathione depletion with DMF/BSO treatment, were performed. This strategy improves the role of glutathione in which the endogenous rate depends on the cell line. ROS is an important factor in the apoptotic process. In our cell models, ROS generation was confirmed by measurement using fluorescent probe CM-H2DCFH-DA, which indicated an overproduction of ROS in cells, in accordance with (Fu et al., 2014; Wan et al., 2012; Kansara et al., 2015). The generation of ROS was correlated with the exposure concentration of nanoparticles in the all three cell lines. For macrophage-like THP-1, the ROS generation appeared later than in micro-vascular endothelial cells HPMEC-ST1.6R or the epithelial A549 cells, in which a burst of ROS was measured earlier as for as 4TiO_2-NPs physiological functionclean off particles in lungs (Oberdörster et al., 1992). Cellular uptake mechanism is important in macrophage. ROS may impact macrophage functions and in part help to drive a chronic inflammatory state observed in some pulmonary diseases (Kirkham, 2007). Direct observation of ROS generation showed that modulation of endogenous redox state by using NAC or DMF/BSO adjuvant treatments had an effect on intracellular ROS levels, demonstrating that the supplementation and depletion strategy was efficient. In the three cell lines, glutathione effectively acted in protection of cells against oxidative stress induced by nanoparticles,

Same supplementation or depletion strategy was involved in cytotoxicity studies (MTS assays and Apoptosis/necrosis measurements). The epithelial A549 cells were highly resistant to TiO_2-NPs exposure as they did not undergo apoptosis, consistent with previous reports (Tedja et al., 2011; Wan et al., 2012; Kansara et al., 2015), even in case of glutathione depletion. Such resistance may be due to physiological function, considering that epithelial cell have to suffer from air exposure in lung and hypoxic modification through the alveolary-capillary barrier. The macrophage-like THP-1 cells were resistant to TiO_2-NPs alone, but a glutathione depletion favored induction of cell death, suggesting potential role of antioxidant protection in cell response. Micro-vascular endothelial cells HPMEC-ST1.6R

ACCEPTED MANUSCRIPT

were the most sensitive cells to TiO_2-NPs, as shown by significant apoptosis induction after exposition to a low dose of TiO_2-NPs (50 µg/ml). This induction of cell death further increased when cells were depleted in their glutathione content. Apoptosis was confirmed with the cleavage of caspase 3 and PARP, observed by western blot. Therefore, here, we determined that cell death response was mainly apoptosis, and demonstrated for the first time that endogenous glutathione level could impact this nanotoxicity response. The dose–dependent cell death response suggested a direct relationship between TiO_2-NPs and oxidative stress response as previously reported (Fu et al., 2014). Moreover, endogenous glutathione may have a major role in cell response, but addition of scavenger as NAC, did not protect cells more in term of cytotoxicity. Finally, A549 are resistant and not sensitive to a variation of their endogenous redox status, unlike the other two cell lines, HPMEC-ST1.6R and THP-1 which were sensitive to changes in endogenous redox state. Although the endogenous glutathione plays a major role, other factors seem to impact the cellular response and behavior.

The known damages induced by ROS overproduction in cell function includes DNA strand breaks or modulation of gene expression through activation of redox-sensitive transcription factors, and modulation of inflammatory responses through signal transduction, leading to cell death and genotoxic effects (Fu et al., 2014). In our study, the A549 cells displayed an endogenous ROS generation, but no repair protein activation, as previously noted concerning H2aX, ATM and P53 phosphorylation (Wan et al., 2012). In A549 cells, NPs-induced ROS did not lead to DNA damage in the time course studied. In HPMEC-ST1.6R and THP-1 cell lines, the persistence of γH2AX protein 24h after treatment demonstrated the recruitment and activation of proteins implied in DNA repair and highlighted the potentiation of cytotoxic and genotoxic risk at local scale (Kumar and Dhawan, 2013). THP-1 cells also displayed activation of DNA repair systems through the phosphorylation of ATM and ATR protein, suggesting that repair processes were still occurring 24 h after exposure. Otherwise, HPMEC-ST1.6R cell line exhibited P53 and Chk1 phosphorylation, consistently with the S-

ACCEPTED MANUSCRIPT

phase arrest of the cell cycle, which was therefore Chk1-dependent. Such cell cycle arrest confirmed the persistence of DNA damage. The p53 pathway also responded to stresses that can disrupt the fidelity of DNA replication and cell division, resulting in the activation of the p53 protein as a transcription factor that initiates a program of cell cycle arrest and cellular apoptosis (Harris and Levine, 2005; Chen and Poon, 2008).

Stress signaling explored through western blotting assays allowed even more to make the link between ROS generation and signaling. The various endpoints revealed a different pattern for each cell type. One of the pathways explored here, considered the activation of SAPK/JNK and its downstream effector C-jun. The resistant A549 displayed no such activated proteins. Otherwise, this pathway was proved to be enabled in HPMEC-ST1.6R and THP-1 cell lines, both sensitive to an endogenous variation of redox status in term of cytotoxicity and exhibited genotoxicity. Activation of these proteins in our experimental conditions was also concomitant with the persistence of DNA lesions detected by the activation of γH2AX, and may correspond also to apoptotic DNA fragmentation for HPMEC-ST1.6R cells specifically (Sluss and Davis, 2006). The JNK group of protein kinases are generally activated in response to a number of cellular stresses, high osmolarity and oxidation (Ip and Davis, 1998), but may be a major concern in term of promotion of inflammatory response (Manke et al., 2013a, 2013b; Shi et al., 2004). Here, SAPK/JNK activation seems appeared in cell lines sensitive to endogenous variation of redox status.

HSP27 protein is activated in all cell lines, suggesting the activation of P38 pathways (Dorion and Landry, 2002; Zarubin and Han, 2005). During oxidative stress, HSP27 functions as an antioxidant, lowering the levels of ROS by raising levels of intracellular glutathione and lowering the levels of intracellular iron (Vidyasagar et al., 2012). Such residual activation of HSP27 correlated with the ROS overproduction observed in all cell lines for different time lines, making HSP27 a marker of intracellular stress in our conditions. The persistence in time of the activation of HSP27 must be carefully considered in the extent that the protein

ACCEPTED MANUSCRIPT

can be considered as a disease marker (Vidyasagar et al., 2012; Zimmermann et al., 2012), in particular pulmonary fibrosis (Wettstein et al., 2013). The upstream activation of P38 protein, associated to ROS overproduction were known to impact apoptosis induction or cell cycle regulation (Ono and Han, 2000; Taylor et al., 2013), and may also be considered as an important pathway in inflammation (Manke et al., 2013a, 2013b) and pathology of pulmonary hypertension and pulmonary vascular remodeling (Church et al., 2012; Han et al., 2013), as well as microvascular dysfunctions (Wang et al., 2010; Nurkiewicz et al., 2011).

Major events related in the study correspond to relatively high dose exposure that was not related to environnemental conditions. However, at a local scale, in lung, the distribution of nanoparticles is not always homogenous. The existence of hot spot of nanoparticles deposition raises today high concern (Donaldson and Poland, 2012; Qiao et al., 2015; Veranth et al., 2010). Considering this, our results showed the activation of protein markers that may be related to pathology. The definition of a hot spot definition has now to be improved to consider local events potentially leading to medical condition.

Conclusion:

ROS generation suggested their role in inducing oxidative stress leading to DNA damage in most treated cells. It is contemplated that the differential susceptibility of cell types could be due to differences in their antioxidant enzyme machinery, metabolic rate, and DNA repair capabilities, which may exhibit variability in TiO_2-NPs induced toxic effects on human health. NPs-induced oxidative stress responses are finally signal transducer for further physiological effects including genotoxicity, inflammation, and fibrosis as demonstrated by activation of associated cell signaling pathways. Since oxidative stress is one of key determinant of NPs-induced injury, it is necessary to characterize the ROS response resulting from NPs. Through understanding of the multiple signaling cascades activated by NPs-induced ROS, a predictive model for NPs-induced injury with oxidative stress could be developed. The overall results of this study offered HSP27 protein as a potential biomarker of intracellular stress and SAPK/JNK as a potential biomarker of sensitivity to changes in endogenous redox state,

ACCEPTED MANUSCRIPT

enabling to predict cell characteristics. The continuation of this study is at date in progress to confirm these roles markers *in vivo* in rats and potentially make the connection with a medical condition such as pulmonary fibrosis.

Acknowledgements

This work was support by INERIS and the French Ministry for ecology, sustainable development and energy (MEDDE),and FONDATION UTC. We thank Dr. Vera Krump-Konvalinkova and Dr. C.J. Kirkpatrick at The Institute of Pathology, Johannes Gutenberg University, Mainz, Germany for the kind gift of HPMEC-ST1.6R cell line used in this study.

ACCEPTED MANUSCRIPT

ACCEPTED MANUSCRIPT

References

Abraham, R.T., 2004. PI 3-kinase related kinases: “big” players in stress-induced signaling pathways. DNA Repair 3, 883–887. doi:10.1016/j.dnarep.2004.04.002

Ahn, J.Y., Schwarz, J.K., Piwnica-Worms, H., Canman, C.E., 2000. Threonine 68 phosphorylation by ataxia telangiectasia mutated is required for efficient activation of Chk2 in response to ionizing radiation. Cancer Res. 60, 5934–5936.

Albrecht, P., Bouchachia, I., Goebels, N., Henke, N., Hofstetter, H.H., Issberner, A., Kovacs, Z., Lewerenz, J., Lisak, D., Maher, P., Mausberg, A.-K., Quasthoff, K., Zimmermann, C., Hartung, H.-P., Methner, A., 2012. Effects of dimethyl fumarate on neuroprotection and immunomodulation. J. Neuroinflammation 9, 163. doi:10.1186/1742-2094-9-163

Baan, R., Straif, K., Grosse, Y., Secretan, B., El Ghissassi, F., Cogliano, V., WHO International Agency for Research on Cancer Monograph Working Group, 2006. Carcinogenicity of carbon black, titanium dioxide, and talc. Lancet Oncol. 7, 295–296.

Boivin, A., Hanot, M., Malesys, C., Maalouf, M., Rousson, R., Rodriguez-Lafrasse, C., Ardail, D., 2011. Transient Alteration of Cellular Redox Buffering before Irradiation Triggers Apoptosis in Head and Neck Carcinoma Stem and Non-Stem Cells. Plos One 6, e14558. doi:10.1371/journal.pone.0014558

Buchmüller-Rouiller, Y., Corrandin, S.B., Smith, J., Schneider, P., Ransijn, A., Jongeneel, C.V., Mauël, J., 1995. Role of glutathione in macrophage

ACCEPTED MANUSCRIPT

activation: effect of cellular glutathione depletion on nitrite production and leishmanicidal activity. Cell. Immunol. 164, 73–80.

Byrne, J.D., Baugh, J.A., 2008. The significance of nanoparticles in particle-induced pulmonary fibrosis. McGill J. Med. MJM 11, 43–50.

Chanput, W., Mes, J.J., Wichers, H.J., 2014. THP-1 cell line: an in vitro cell model for immune modulation approach. Int. Immunopharmacol. 23, 37–45. doi:10.1016/j.intimp.2014.08.002

Chen, T., Yan, J., Li, Y., 2014. Genotoxicity of titanium dioxide nanoparticles. J. Food Drug Anal. 22, 95–104. doi:10.1016/j.jfda.2014.01.008

Chen, Y., Poon, R.Y.C., 2008. The multiple checkpoint functions of CHK1 and CHK2 in maintenance of genome stability. Front. Biosci. J. Virtual Libr. 13, 5016–5029.

Chen, Z., Wang, Y., Ba, T., Li, Y., Pu, J., Chen, T., Song, Y., Gu, Y., Qian, Q., Yang, J., Jia, G., 2014. Genotoxic evaluation of titanium dioxide nanoparticles in vivo and in vitro. Toxicol. Lett. 226, 314–319. doi:10.1016/j.toxlet.2014.02.020

Church, A.C., Wadsworth, R., Bryson, G., Welsh, D.J., Peacock, A.J., 2012. S36 P38 MAPK: An Important Pathway in the Pathobiology of Pulmonary Hypertension and Pulmonary Vascular Remodelling. Thorax 67, A19–A20. doi:10.1136/thoraxjnl-2012-202678.042

Donaldson, K., Poland, C.A., 2012. Chapter 7 - Respiratory System, in: Shvedova, B.F.P.A. (Ed.), Adverse Effects of Engineered Nanomaterials. Academic Press, Boston, pp. 121–137.

Dorion, S., Landry, J., 2002. Activation of the mitogen-activated protein kinase pathways by heat shock. Cell Stress Chaperones 7, 200–206.

ACCEPTED MANUSCRIPT

Fahmy, B., Cormier, S.A., 2009. Copper oxide nanoparticles induce oxidative stress and cytotoxicity in airway epithelial cells. Toxicol. Vitro Int. J. Publ. Assoc. BIBRA 23, 1365–1371. doi:10.1016/j.tiv.2009.08.005

Falck, G.C.M., Lindberg, H.K., Suhonen, S., Vippola, M., Vanhala, E., Catalán, J., Savolainen, K., Norppa, H., 2009. Genotoxic effects of nanosized and fine TiO2. Hum. Exp. Toxicol. 28, 339–352. doi:10.1177/0960327109105163

Forman, H.J., Zhang, H., Rinna, A., 2009. Glutathione: overview of its protective roles, measurement, and biosynthesis. Mol. Aspects Med. 30, 1–12. doi:10.1016/j.mam.2008.08.006

Foster, K.A., Oster, C.G., Mayer, M.M., Avery, M.L., Audus, K.L., 1998. Characterization of the A549 cell line as a type II pulmonary epithelial cell model for drug metabolism. Exp. Cell Res. 243, 359–366. doi:10.1006/excr.1998.4172

Fu, P.P., Xia, Q., Hwang, H.-M., Ray, P.C., Yu, H., 2014. Mechanisms of nanotoxicity: generation of reactive oxygen species. J. Food Drug Anal. 22, 64–75. doi:10.1016/j.jfda.2014.01.005

Hanot, M., Boivin, A., Malesys, C., Beuve, M., Colliaux, A., Foray, N., Douki, T., Ardail, D., Rodriguez-Lafrasse, C., 2012. Glutathione Depletion and Carbon Ion Radiation Potentiate Clustered DNA Lesions, Cell Death and Prevent Chromosomal Changes in Cancer Cells Progeny. Plos One 7, e44367. doi:10.1371/journal.pone.0044367

Han, S.G., Newsome, B., Hennig, B., 2013. Titanium dioxide nanoparticles increase inflammatory responses in vascular endothelial cells. Toxicology 306, 1–8. doi:10.1016/j.tox.2013.01.014

ACCEPTED MANUSCRIPT

Harris, S.L., Levine, A.J., 2005. The p53 pathway: positive and negative feedback loops. Oncogene 24, 2899–2908. doi:10.1038/sj.onc.1208615

Huang Yue-Wern, W.C., 2010. Toxicity of Transition Metal Oxide Nanoparticles: Recent Insights from in vitro Studies. Materials 3. doi:10.3390/ma3104842

IARC, 2010. IARC monographs on the evaluation of carcinogenic risks to humans: carbon black, titanium dioxide, and talc. Lyon Fr. World Health Organ. Int. Agency Res. Cancer 93.

Iavicoli, I., Leso, V., Fontana, L., Bergamaschi, A., 2011. Toxicological effects of titanium dioxide nanoparticles: a review of in vitro mammalian studies. Eur. Rev. Med. Pharmacol. Sci. 15, 481–508.

Ip, Y.T., Davis, R.J., 1998. Signal transduction by the c-Jun N-terminal kinase (JNK)--from inflammation to development. Curr. Opin. Cell Biol. 10, 205–219.

Kansara, K., Patel, P., Shah, D., Shukla, R.K., Singh, S., Kumar, A., Dhawan, A., 2015. TiO2 nanoparticles induce DNA double strand breaks and cell cycle arrest in human alveolar cells. Environ. Mol. Mutagen. 56, 204–217. doi:10.1002/em.21925

Kerksick, C., Willoughby, D., 2005. The Antioxidant Role of Glutathione and N-Acetyl-Cysteine Supplements and Exercise-Induced Oxidative Stress. J. Int. Soc. Sports Nutr. 2, 38–44. doi:10.1186/1550-2783-2-2-38

Kirkham, P., 2007. Oxidative stress and macrophage function: a failure to resolve the inflammatory response. Biochem. Soc. Trans. 35, 284–287. doi:10.1042/BST0350284

Krump-Konvalinkova, V., Bittinger, F., Unger, R.E., Peters, K., Lehr, H.-A., Kirkpatrick, C.J., 2001. Generation of Human Pulmonary Microvascular

ACCEPTED MANUSCRIPT

Endothelial Cell Lines. Lab. Invest. 81, 1717–1727. doi:10.1038/labinvest.3780385

Kumar, A., Dhawan, A., 2013. Genotoxic and carcinogenic potential of engineered nanoparticles: an update. Arch. Toxicol. 87, 1883–1900. doi:10.1007/s00204-013-1128-z

Lane, D.P., 1992. Cancer. p53, guardian of the genome. Nature 358, 15–16. doi:10.1038/358015a0

Lanone, S., Rogerieux, F., Geys, J., Dupont, A., Maillot-Marechal, E., Boczkowski, J., Lacroix, G., Hoet, P., 2009. Comparative toxicity of 24 manufactured nanoparticles in human alveolar epithelial and macrophage cell lines. Part. Fibre Toxicol. 6, 14. doi:10.1186/1743-8977-6-14

Lee, M., Cho, T., Jantaratnotai, N., Wang, Y.T., McGeer, E., McGeer, P.L., 2010. Depletion of GSH in glial cells induces neurotoxicity: relevance to aging and degenerative neurological diseases. FASEB J. 24, 2533–2545. doi:10.1096/fj.09-149997

Leung, S.W., Mitchell, J.B., al-Nabulsi, I., Friedman, N., Newsome, J., Belldegrun, A., Kasid, U., 1993. Effect of L-buthionine sulfoximine on the radiation response of human renal carcinoma cell lines. Cancer 71, 2276–2285.

Lewis-Wambi, J.S., Swaby, R., Kim, H., Jordan, V.C., 2009. Potential of l-buthionine sulfoximine to enhance the apoptotic action of estradiol to reverse acquired antihormonal resistance in metastatic breast cancer. J. Steroid Biochem. Mol. Biol. 114, 33–39. doi:10.1016/j.jsbmb.2008.12.016

Lin, W., Stayton, I., Huang, Y., Zhou, X.-D., Ma, Y., 2008. Cytotoxicity and cell membrane depolarization induced by aluminum oxide nanoparticles in human

ACCEPTED MANUSCRIPT

lung epithelial cells A549. Toxicol. Environ. Chem. 90, 983–996. doi:10.1080/02772240701802559

Lu, X., Zhu, T., Chen, C., Liu, Y., 2014. Right or left: the role of nanoparticles in pulmonary diseases. Int. J. Mol. Sci. 15, 17577–17600. doi:10.3390/ijms151017577

Madl, A.K., Plummer, L.E., Carosino, C., Pinkerton, K.E., 2014. Nanoparticles, Lung Injury, and the Role of Oxidant Stress. Annu. Rev. Physiol. 76, 447–465. doi:10.1146/annurev-physiol-030212-183735

Manke, A., Wang, L., Rojanasakul, Y., 2013a. Mechanisms of nanoparticle-induced oxidative stress and toxicity. BioMed Res. Int. 2013, 942916. doi:10.1155/2013/942916

Manke, A., Wang, L., Rojanasakul, Y., 2013b. Pulmonary toxicity and fibrogenic response of carbon nanotubes. Toxicol. Mech. Methods 23, 196–206. doi:10.3109/15376516.2012.753967

Martinho, R.G., Lindsay, H.D., Flaggs, G., DeMaggio, A.J., Hoekstra, M.F., Carr, A.M., Bentley, N.J., 1998. Analysis of Rad3 and Chk1 protein kinases defines different checkpoint responses. EMBO J. 17, 7239–7249. doi:10.1093/emboj/17.24.7239

Matsuoka, S., Rotman, G., Ogawa, A., Shiloh, Y., Tamai, K., Elledge, S.J., 2000. Ataxia telangiectasia-mutated phosphorylates Chk2 in vivo and in vitro. Proc. Natl. Acad. Sci. U. S. A. 97, 10389–10394. doi:10.1073/pnas.190030497

Mirowsky, J.E., Jin, L., Thurston, G., Lighthall, D., Tyner, T., Horton, L., Galdanes, K., Chillrud, S., Ross, J., Pinkerton, K.E., Chen, L.C., Lippmann, M., Gordon, T., 2015. In vitro and in vivo toxicity of urban and rural particulate matter from

ACCEPTED MANUSCRIPT

California. Atmospheric Environ. Oxf. Engl. 1994 103, 256–262. doi:10.1016/j.atmosenv.2014.12.051

Nurkiewicz, T.R., Porter, D.W., Hubbs, A.F., Stone, S., Moseley, A.M., Cumpston, J.L., Goodwill, A.G., Frisbee, S.J., Perrotta, P.L., Brock, R.W., Frisbee, J.C., Boegehold, M.A., Frazer, D.G., Chen, B.T., Castranova, V., HEI Health Review Committee, 2011. Pulmonary particulate matter and systemic microvascular dysfunction. Res. Rep. Health Eff. Inst. 3–48.

Oberdörster, G., Ferin, J., Gelein, R., Soderholm, S.C., Finkelstein, J., 1992. Role of the alveolar macrophage in lung injury: studies with ultrafine particles. Environ. Health Perspect. 97, 193–199.

Ono, K., Han, J., 2000. The p38 signal transduction pathway: activation and function. Cell. Signal. 12, 1–13.

Onuma, K., Sato, Y., Ogawara, S., Shirasawa, N., Kobayashi, M., Yoshitake, J., Yoshimura, T., Iigo, M., Fujii, J., Okada, F., 2009. Nano-scaled particles of titanium dioxide convert benign mouse fibrosarcoma cells into aggressive tumor cells. Am. J. Pathol. 175, 2171–2183. doi:10.2353/ajpath.2009.080900

Park, E.-J., Yi, J., Chung, K.-H., Ryu, D.-Y., Choi, J., Park, K., 2008. Oxidative stress and apoptosis induced by titanium dioxide nanoparticles in cultured BEAS-2B cells. Toxicol. Lett. 180, 222–229. doi:10.1016/j.toxlet.2008.06.869

Pouliliou, S., Koukourakis, M.I., 2014. Gamma histone 2AX (γ-H2AX)as a predictive tool in radiation oncology. Biomark. Biochem. Indic. Expo. Response Susceptibility Chem. 19, 167–180. doi:10.3109/1354750X.2014.898099

Qiao, H., Liu, W., Gu, H., Wang, D., Wang, Y., Qiao, H., Liu, W., Gu, H., Wang, D., Wang, Y., 2015. The Transport and Deposition of Nanoparticles in Respiratory System by Inhalation, The Transport and Deposition of Nanoparticles in

ACCEPTED MANUSCRIPT

Respiratory System by Inhalation. J. Nanomater. J. Nanomater. 2015, 2015, e394507. doi:10.1155/2015/394507, 10.1155/2015/394507

Rogakou, E.P., Pilch, D.R., Orr, A.H., Ivanova, V.S., Bonner, W.M., 1998. DNA double-stranded breaks induce histone H2AX phosphorylation on serine 139. J. Biol. Chem. 273, 5858–5868.

Rollerova, E., Tulinska, J., Liskova, A., Kuricova, M., Kovriznych, J., Mlynarcikova, A., Kiss, A., Scsukova, S., 2015. Titanium dioxide nanoparticles: some aspects of toxicity/focus on the development. Endocr. Regul. 49, 97–112.

Shechter, D., Costanzo, V., Gautier, J., 2004. Regulation of DNA replication by ATR: signaling in response to DNA intermediates. DNA Repair 3, 901–908. doi:10.1016/j.dnarep.2004.03.020

Shieh, S.Y., Ikeda, M., Taya, Y., Prives, C., 1997. DNA damage-induced phosphorylation of p53 alleviates inhibition by MDM2. Cell 91, 325–334.

Shi, H., Hudson, L.G., Liu, K.J., 2004. Oxidative stress and apoptosis in metal ion-induced carcinogenesis. Free Radic. Biol. Med. 37, 582–593. doi:10.1016/j.freeradbiomed.2004.03.012

Shi, H., Magaye, R., Castranova, V., Zhao, J., 2013. Titanium dioxide nanoparticles: a review of current toxicological data. Part. Fibre Toxicol. 10, 15. doi:10.1186/1743-8977-10-15

Sluss, H.K., Davis, R.J., 2006. H2AX is a target of the JNK signaling pathway that is required for apoptotic DNA fragmentation. Mol. Cell 23, 152–153. doi:10.1016/j.molcel.2006.07.001

Taylor, C.A., Zheng, Q., Liu, Z., Thompson, J.E., 2013. Role of p38 and JNK MAPK signaling pathways and tumor suppressor p53 on induction of apoptosis in

ACCEPTED MANUSCRIPT

response to Ad-eIF5A1 in A549 lung cancer cells. Mol. Cancer 12, 35. doi:10.1186/1476-4598-12-35

Tedja, R., Marquis, C., Lim, M., Amal, R., 2011. Biological impacts of TiO2 on human lung cell lines A549 and H1299: particle size distribution effects. J. Nanoparticle Res. 13, 3801–3813. doi:10.1007/s11051-011-0302-6

Veranth, J.M., Ghandehari, H., Grainger, D.W., 2010. 8.23 - Nanoparticles in the Lung, in: McQueen, C.A. (Ed.), Comprehensive Toxicology (Second Edition). Elsevier, Oxford, pp. 453–475.

Vidyasagar, A., Wilson, N.A., Djamali, A., 2012. Heat shock protein 27 (HSP27): biomarker of disease and therapeutic target. Fibrogenesis Tissue Repair 5, 7. doi:10.1186/1755-1536-5-7

Wang, T., Chiang, E.T., Moreno-Vinasco, L., Lang, G.D., Pendyala, S., Samet, J.M., Geyh, A.S., Breysse, P.N., Chillrud, S.N., Natarajan, V., Garcia, J.G.N., 2010. Particulate matter disrupts human lung endothelial barrier integrity via ROS- and p38 MAPK-dependent pathways. Am. J. Respir. Cell Mol. Biol. 42, 442–449. doi:10.1165/rcmb.2008-0402OC

Wang, Y., He, Y., Lai, Q., Fan, M., 2014. Review of the progress in preparing nano TiO2: an important environmental engineering material. J. Environ. Sci. China 26, 2139–2177. doi:10.1016/j.jes.2014.09.023

Wan, R., Mo, Y., Feng, L., Chien, S., Tollerud, D.J., Zhang, Q., 2012. DNA damage caused by metal nanoparticles: involvement of oxidative stress and activation of ATM. Chem. Res. Toxicol. 25, 1402–1411. doi:10.1021/tx200513t

Warheit, D.B., Donner, E.M., 2015. Risk assessment strategies for nanoscale and fine-sized titanium dioxide particles: Recognizing hazard and exposure issues.

ACCEPTED MANUSCRIPT

Food Chem. Toxicol. Int. J. Publ. Br. Ind. Biol. Res. Assoc. 85, 138–147. doi:10.1016/j.fct.2015.07.001

Weinberg, F., Hamanaka, R., Wheaton, W.W., Weinberg, S., Joseph, J., Lopez, M., Kalyanaraman, B., Mutlu, G.M., Budinger, G.R.S., Chandel, N.S., 2010. Mitochondrial metabolism and ROS generation are essential for Kras-mediated tumorigenicity. Proc. Natl. Acad. Sci. U. S. A. 107, 8788–8793. doi:10.1073/pnas.1003428107

Wettstein, G., Bellaye, P.-S., Kolb, M., Hammann, A., Crestani, B., Soler, P., Marchal-Somme, J., Hazoume, A., Gauldie, J., Gunther, A., Micheau, O., Gleave, M., Camus, P., Garrido, C., Bonniaud, P., 2013. Inhibition of HSP27 blocks fibrosis development and EMT features by promoting Snail degradation. FASEB J. Off. Publ. Fed. Am. Soc. Exp. Biol. 27, 1549–1560. doi:10.1096/fj.12-220053

Yan, S., Sorrell, M., Berman, Z., 2014. Functional interplay between ATM/ATR-mediated DNA damage response and DNA repair pathways in oxidative stress. Cell. Mol. Life Sci. CMLS 71, 3951–3967. doi:10.1007/s00018-014-1666-4

Zarubin, T., Han, J., 2005. Activation and signaling of the p38 MAP kinase pathway. Cell Res. 15, 11–18. doi:10.1038/sj.cr.7290257

Zimmermann, M., Nickl, S., Lambers, C., Hacker, S., Mitterbauer, A., Hoetzenecker, K., Rozsas, A., Ostoros, G., Laszlo, V., Hofbauer, H., Renyi-Vamos, F., Klepetko, W., Dome, B., Ankersmit, H.J., 2012. Discrimination of clinical stages in non-small cell lung cancer patients by serum HSP27 and HSP70: a multi-institutional case-control study. Clin. Chim. Acta Int. J. Clin. Chem. 413, 1115–1120. doi:10.1016/j.cca.2012.03.008

ACCEPTED MANUSCRIPT

Table 1

A

% Apoptotic cells ± SD

	[NPs] µg/ml	Ø	+ NAC	+ DMF/BSO
THP-1	0	2,2 ± 3,7	1,2 ± 1,1	5,0 ± 3,7
	5	4,5 ± 3,9	3,2 ± 5,3	**14,0 ± 4,4** [a b]
	200	4,9 ± 3,5	5,3 ± 4,3	**20,2 ± 5,1** [a b]
	800	6,3 ± 3,7	4,4 ± 3,9	**33,9 ± 5,9** [a b]
A549	0	2,3 ± 1,8	0,1 ± 0,0	1,5 ± 2,0
	5	2,6 ± 2,3	0,6 ± 0,8	2,6 ± 0,8
	200	2,9 ± 0,6	1,3 ± 1,8	3,6 ± 0,6
	800	5,3 ± 3,1	3,1 ± 1,6	2,9 ± 0,7
HPMEC	0	2,0 ± 2,5	1,5 ± 0,7	3,2 ± 0,8
	5	**9,3 ± 2,5** [a]	5,5 ± 0,8 [a]	**19,5 ± 0,8** [a b]
	200	**13,7 ± 1,4** [a]	13,8 ± 1,6 [a]	**24,9 ± 5,2** [a b]
	800	**19,8 ± 3,4** [a]	15,5 ± 2,4 [a]	**41,0 ± 3,4** [a b]

B

% Necrotic cells ± SD

	[NPs] µg/ml	Ø	+ NAC	+ DMF/BSO
THP-1	0	0,1 ± 0,0	0,2 ± 0,2	1,1 ± 1,0
	5	2,1 ± 1,2	1,1 ± 1,3	1,3 ± 1,1
	200	2,9 ± 1,2	3,7 ± 2,2	3,0 ± 1,1
	800	2,0 ± 2,0	1,5 ± 1,2	4,9 ± 3,4
A549	0	0,8 ± 0,5	0,8 ± 0,1	1,1 ± 0,5
	5	1,5 ± 1,3	0,0 ± 0,0	1,3 ± 1,6
	200	2,1 ± 0,9	2,9 ± 0,4	3,0 ± 1,5
	800	1,3 ± 1,6	4,2 ± 1,5	4,9 ± 1,8
HPMEC	0	2,7 ± 1,1	0,9 ± 0,5	3,1 ± 0,7
	5	2,2 ± 1,7	2,0 ± 2,9	3,0 ± 0,8
	200	2,1 ± 1,0	2,7 ± 0,3	3,3 ± 1,0
	800	2,9 ± 1,6	3,3 ± 0,8	4,6 ± 0,5

ACCEPTED MANUSCRIPT

Highlights

► Nanoparticles-exposed cell lines showed ROS generation, a common toxicity mechanism

► Alveolar epithelial A549 were resistant to nanoparticles exposure

► HPMEC-ST1.6R and THP-1 cells were sensitive to endogenous redox changes

► Correlation between cyto- and geno-toxicological endpoints and oxidative stress activated pathways

► HSP27 and SAPK/JNK proteins were potential markers to predict cell response

ACCEPTED MANUSCRIPT